



## Flexural behaviour of reinforced concrete beams strengthened by NSM technique using ECC

Fady Awad, Mohamed Husain, Khaled Fawzy

Faculty of Engineering, University of Zagazig, Zagazig, Egypt.

Civfadyawad@gmail.com, <https://orcid.org/0000-0001-7600-5690>

Mo\_husain2000@yahoo.com.

khaleed\_lashen1@yahoo.com, <https://orcid.org/0000-0003-2275-4025>

**ABSTRACT.** Bendable concrete is also defined as engineered cementitious composites (ECC) because of its excellent flexibility and tight fracture width limitation. ECC is a mixture of the addition of Portland cement, silica sand, fly ash, and fiber types (polypropylene (PP) and polyvinyl alcohol (PVA)). The main objective of the research is to investigate the bending performance of a series of reinforced concrete (RC) beams. Which were externally bonded (EB) with steel bars using a near-surface mounted technique with ECC or Epoxy, and we came out with a result, which is the best method of strengthening used in this test. A total of 5 RC beams of 1500 mm in length, 150 mm in width, and 200 mm in height - including one control and four - were strengthened, prepared, and tested. The varied test parameters are the ECC mortar, Epoxy, and the different shapes of strengthening cross-section. The test results revealed that ECC is an ideal cement matrix for reinforcement applications where ECC mortar bonded with steel bars is used as external reinforcement. As a result, ECC has many attractive properties, such as high tensile ductility compared to ordinary concrete while maintaining compressive strength.

**KEYWORDS.** RC beam; Flexural strengthening; Engineered Cementitious Composites (ECC); Near Surface Mounted (NSM); ANSYS; Ductility.



**Citation:** Awad, F., Husain, M., Fawzy, K., Flexural behaviour of reinforced concrete beams strengthened by NSM technique using ECC, *Frattura ed Integrità Strutturale*, 60 (2022) 291-309.

**Received:** 02.12.2021

**Accepted:** 10.02.2022

**Online first:** 27.02.2022

**Published:** 01.04.2022

**Copyright:** © 2022 This is an open access article under the terms of the CC-BY 4.0, which permits unrestricted use, distribution, and reproduction in any medium, provided the original author and source are credited.

### INTRODUCTION

The strengthening of established concrete members' technologies has gained considerable interest in civil engineering culture over the past fifty years. However, concrete carbonation and free-thaw replication resulting from long-term environmental factors could undermine concrete structures. In addition, as time progresses, current concrete systems could suffer progressive damage (or fatigue) due to repeated loading. Therefore, modifying existing structures rather than demolition or new construction is preferable to reduce construction waste and construction costs. Thus, cost-effective and easy-to-install retrofit methods for existing structural members have been developed and have received attention.

Concretes that have been used in the past are nearly unbendable, rendering them incredibly brittle and stiff with a strain potential of just 0.1 percent. This lack of bendability is a significant cause of stress failure; it has been a guiding force creating an elegant substance called bendable concrete. This composite is capable of showing substantially improved versatility. The bendable concrete is reinforced with silicone fibers that are micro mechanically engineered. Among these materials, ECC mortar can dramatically show substantially enhanced versatility. Because ECC has a greater than 3% strain potential, it has the properties of ductile metal rather than brittle glass. Micro-mechanically produced polymer fibers are used to support bendable concrete.

ECC is made from the same essential elements as regular concrete, but it is vital to have good workability with a high-range water reduction (HRWR) agent. On the other hand, coarse aggregates are not employed in ECCs (hence it is a mortar rather than concrete). As a result, ECC has a relatively high powder content. To improve the paste content, cementitious materials such as silica sand, fly ash, blast slag, silica fume, and so on can be added to the cement. ECC also uses tiny cutting fibers (usually 2% by volume), fine silica sand, and fly ash. This surface coating causes the fiber to start sliding when overloaded, not crack [1].



Figure 1: Response of ECC under Flexural Loading.

The ductility of a concrete element can be employed as a measure of a structural member's or system's resistance to deformation during the transition from until collapse, the elastic zone to the plastic zone. Ductility is characterized as the ability to withstand inelastic deformations without substantial strength loss before failure, which is a critical design prerequisite in most RC structures design codes. Fig. (1) shows the observed plate ductility. As a result, ductility is now a required function of modern structural architecture to prevent a fragile collapse of structures, ensuring massive plastic deformation and avoiding extreme harm under complex loads. The ductility index is a method of assessing the ductility of structural components. In terms of ductility, the effects of employing ECC to strengthen RC beams are highly effective.

NSM (Near Surface Mounted) Some traditional reinforcement strategies for deteriorated concrete structures are bonding. The NSM device will stabilize existing concrete frameworks with less labor and without changing their proportions. The post-tension NSM method was implemented to increase the bendable ability of concrete buildings that are weakened due to aging or the natural environment. Many approaches can implement that technique. Generally, the lowest face of the concrete pillar is wrapped with a repairing sheet bonded to the beam's stress face. The resilience of structural members can be improved, even after they have been badly weakened due to loading conditions.

In the state of any failure of reinforced concrete members, this would necessitate first repairing the member by clearing loose debris and filling holes and fractures with Epoxy mortar or ECC. ECC will be employed in this research. Engineered Cementitious Composites are a type of ultra-high-strength-concrete (UHSC). It's a group of high-performance fiber-reinforced cement composites with high tensile ductility showing up in hybrid steel-concrete systems that are exceptionally resistant to cracking and can handle bonding stresses better than ordinary concrete structures.

## LITERATURE REVIEW

Literature review of previous work presented as below.

S.M. Gadhiya [2]. Find out flexural strength, compressive strength, and deflection characteristics for different types of fibers for different beam depths. ECC's expansion capacity is over 3%, so it behaves more like a ductile metal than a brittle glass. A comparison study was carried out on the fresh and hardened properties of concrete for different fibers, and specimen deflection concerning the depth of the specimen found. The density of ECC is 20% lower than Conventional



Concrete. Flexural strength and deflection are inversely related to the cross-section area of the specimen. ECC with increasing fibers' increases about 20% of Energy Absorption, whereas by increasing the cross-section of the specimen, 10% increment in Energy absorption is evaluated.

Jian Zhou et al. [3]. Compared to the experimental findings of the uniaxial tensile test and the fiber diffusion analysis, the effect of various water mixing sequences was studied, experimented with enhanced fiber delivery by changing the sequence of mixing. With the normal mixing series, fibers are added after both solid and liquid materials are combined. Undesirable plastic viscosity can lead to poor fiber distribution and poor curing properties until the fibers adhere. The connection of solid and liquid materials is divided into two phases with modified mixing sequences, and fiber incorporation is between the two steps. The result was that the modified mixing sequence increases the tensile strain potential and ultimate tensile strength of ECC relative to the normal mixing sequence and improves fiber distribution.

Mustafa Sahmaran et al. [4]. Study The effect of the high concentrations of fly ash and small size of poly-vinyl-alcohol (PVA) fibers on the cyclic freeze-thaw tolerance and the microstructure of the Manufactured Cementitious Composites has been experimentally tested. ECC mixtures were prepared with two different ratios of FA-cement (FA/C) (1.2 and 2.2 by weight) and with a constant ratio of 0.27 for water-cement products (fly ash and cement). The assessment of residual mechanical features requires laboratory experiments like (flexural strength, mid-span beam deflection, and flexural stress-deflection curve). The findings indicate that all ECC mixtures with super-high Fly Ash volumes remain stable and show a tensile strain potential of more than 2% even after 300 freezing and thawing cycles. The results showed that ECC mixtures with a FA/C ratio of 2.2 showed that the reduction of residual physical and mechanical properties with an increasing number of freeze-thaw cycles is comparatively more than ECC mixtures with a FA/C ratio of 1.2.

ECC products have been studied for their ability to self-heal [5]. The crack features of M45 and HFA-ECC specimens pre-loaded to strain levels of 0.3 percent, 0.5 percent, 1.0 percent, and 2.0 percent were investigated. The operation was done at various ages, including resonance frequencies, mechanical recovery of re-healed ECC materials, new crack pathways after reloading, and chemical examination of healing goods. The self-healing actions of ECC with multiple micro-cracks benefit based on the experimental results. Longer samples of aged and high fly ash lead to smaller cracks forming.

Jun Zhang et al. [6]. The possible applications of the Low Drying Shrinkage Characteristic (LSECC) fiber-reinforced engineered cement composite in concrete pavements for the removal of joints usually used to tolerate temperature and shrinkage deformation are noted. So instead of cracking in the adjacent concrete slab, a hybrid slab consisting of both plain concrete and LSECC, with LSECC/concrete interface steel bars and engineered building procedures, was found to distinguish the tensile cracks in the LSECC strip. Because of the strain-hardening and high strain capacity of the LSECC, the integrity of the composite slab and total strain capacity can be considerably increased. Shrinkage deformations and temperature can be addressed by properly selecting the LSECC strip and concrete slab length ratio.

S.Z. Qian et al. [7]. The self-healing action of Engineered Cementitious Composites (ECC) was studied with an emphasis on the impact of curing conditions and pre-cracking time. Four-point bending experiments were used to pre-crack ECC beams at varying ages, followed by multiple curing conditions, including air curing, 3 percent CO<sub>2</sub> concentration curing, cyclic wet/dry (dry below 3 percent CO<sub>2</sub> concentration) curing, and water curing. Flexural stiffness has also been greatly preserved during self-healing relative to that of virgin samples, but the degree of retention declines with the rise in pre-cracking time. For samples pre-cracked at the age of 14 days and 28 days, the flexural strength improves, possibly due to constant hydration of cement products afterward. In addition, the use of Nano-clay as dispersed internal water sources to facilitate self-healing actions within ECC without depending on external water supply was encouraging.

Gabriel Jen et al. [8]. To observe the reduction in corrosion risk of self-consolidated hybrid fiber reinforced concrete, experimental work has been carried out. There have been correlations between the incidence of corrosion damage in reinforced concrete and noticeable cracking defined by a multitude of construction codes. The role of crack suppression in corrosion damage initiation and propagation stages is investigated using a self-consolidated hybrid fiber reinforced concrete mixture in a chloride-induced corrosion environment. It is observed that in the presence of hybrid fiber reinforcement, in contrast to traditional concrete tests, chloride migration rates are not significantly modified by the application of moderate cyclical mechanical loading. An improved measure of durability is given by hybrid fiber reinforcement.

Jung et al. [9]. They performed an experimental investigation on the flexural behavior of RC beams strengthened with near-surface mounted (NSM) carbon fiber reinforced polymer (CFRP) reinforcement. Two CFRP strips were examined, namely 21 mm<sup>2</sup> and 35 mm<sup>2</sup>. They reported that the NSM strengthened specimens utilized the CFRP reinforcement more efficiently than externally bonded strengthened beams.

D. Novidis et al. [10]. The bond behavior of NSM bars was tested experimentally; two failure modes were observed: failure of the concrete epoxy interface and failure occurred of the bar-epoxy interface. The test results revealed that average bond strength improves as failure is regulated by the bar and epoxy paste interface, increasing the groove size. Additionally, for a given groove size, increasing the bonded length increased the load capacity of the joint.

Jang et al. [9]. They presented an analytical evaluation of RC beams strengthened with NSM strips. The study focused on the relation between the ultimate strength and the depth of the NSM groove size and the spacing between the CFRP strips. They reported that the minimum spacing between the NSM groove (for multiple numbers of CFRP strips) and from the edge of the beam should exceed 40 mm to ensure that each CFRP strip behaved independently.

Sabaa et Al. [11]. Workability has been stated as a very significant concrete property that will influence the rate of placement and the degree of concrete compaction.

En-Hua Yang et al. [12]. Four variables were used in their analysis, such as Class C Fly ash ratio to Class F Fly ash ratio, water to binder ratio, High-range water reducer quantity, and Viscosity Changing Admixture quantity, to examine the structure effects of ECC on fresh and hardened properties.

Dhawale et al. [13]. Melamine-based super-plasticizer has been stated to be the best plasticizer and hence selected for the research work. Melamine Formaldehyde Sulphonate was the super-plasticizer used. The original mix ratio was 1:0.80, PVA fiber 1% and the super-plasticizer dosage was 1040.47ml/bag, and the ratio of water to cement content was 0.274. But workability was not reached by using this proportion. Studies conducted by several authors on the development and commercialization of engineered cementitious composites (ECC) have proven to be one of the best alternatives and most sustainable concrete materials in the coming decades. I am. Example ECCL70 shows a maximum deflection of 29 mm compared to ECCL5 (19 mm). ECC250, ECC500, ECC750 show 16 mm, 19 mm, and 24 mm, and the control bar is only 14 mm.

Shamsher Bahadur Singh et al. [13]. They Explored the flexural behavior of frame systems made of concrete and ductile fibre reinforced cementitious composites (DFRCC) under rigid transverse bending in their research.

Shang et al. (2019) [14] Studying the strain hardening characteristics and strong interfacial adhesion to concrete, it was found to be an ideal material for structural reinforcement. A formula for calculating the bending resistance of RC girders and the shear resistance of RC columns modified from this composite layer has been proposed. However, the formula for calculating the shear strength of reinforced RC beams is not yet known.

Jin-Keun Kim et al. [15]. They evaluated ECC's stretching and dispersion performance made from crushed blast furnace slag. They used 60%, 48%, 38%, 35% and 28% water binder ratios (W / B) to measure fiber / matrix interfacial properties and mortar matrix fracture toughness. The results show that both ductility and tensile strength of Slag ECC were significantly higher than these values measured with slag-free ECC. The use of slag particles should help achieve work-hardening behavior. Adding slag particles at the same W / C (60%) reduces the toughness ratio, but the tensile stress capacity of Slag ECC is about 50% higher than that of ECC without slag. The contribution of slag particles in ECC improves workability. Via the previous literature, it was identified that ECC is a new constructor material and is considered a good material in traditional construction works due to its good mechanical and physical properties. Therefore, it is preferable to use ECC material over traditional reinforced concrete as a modern, strong structural material in major construction works such as bridges, dams, beams with a wide span, prestressed beams, etc.

In this study, we study ECC as a strengthened material used to strengthen the existing structural elements to know the extent of its exposure and bearing to high loads. we also learn about the best methods of NSM strengthening that give the best results with this material (ECC). The research work aims to study the flexural response of engineered cementitious (ECC) as strengthened material for reinforced concrete beams and compare Epoxy and ECC In terms of bond between strengthening steel bars and RC beams.

## EXPERIMENTAL PROGRAM

### *Specimens Geometry and Reinforcement* [16]

The specimens tested included (5) concrete beam specimens (one control beam, one beam strengthened with kema epoxy 165, and Three beams strengthened with (ECC)) were tested to evaluate the efficiency of ECC in flexure strengthening. The dimensions of all specimens are 1500 mm-long, 150 mm-wide, and 200 mm-deep. The concrete cover thickness was 20 mm. The details of control beam reinforcement are shown in Fig. (3.a). The NSM technique did the flexure strengthening with (kema epoxy 165 once and used ECC) groove size was set at  $1.5d_b \approx 20$  mm. The beam is designed to break in deflection rupture mode. Preparation, casting, curing concrete beams and cubes, and testing process were in laboratories of structural engineering department, Faculty of engineering at Zagazig University by MTS machine, with Capacity 1000 KN. Specimens were tested as a four-point bending test to depict the stress-strain curve and determine the modulus of elasticity, as shown in Fig. (2). All beams are reinforced by 2Ø8 at the top and bottom and stirrups 2Ø8@10 cm. Using at Strengthen 2Ø12 as shown in the following Tab. (1). Tab. (2) illustrates the strengthening scheme of RC beams.



Figure 2: MTS machine, with Capacity 1000KN.

The following table summarize the experimental work.

Beam No.	Reinforced Bars & Stirrups			The form of Strengthen
	Top	Bottom	Stirrups	
Beam 01				Control beam.
Beam 02				2Ø12 + Kema Epoxy 165 with groove (2*2*100) cm.
Beam 03	2Ø8	2Ø8	5Ø8/m'	2Ø12 + ECC groove (2*2*100) cm.
Beam 04				2Ø12 + ECC plate (2*15*100) cm.
Beam 05				2Ø12 + ECC U-plate (5*2) + (2*15*100) cm.

Table 1: Experimental work beams plan.

## MATERIAL PROPERTIES

The materials used in the reinforced concrete specimens for construction and those for strengthening were fine aggregate (sand), coarse aggregate (dolomite), cement, water, steel reinforcement bars, polypropylene fiber (PP), polyvinyl alcohol fiber (PVA), fly ash class(F), fine silica sand, epoxy adhesive (SIKA dur 32) and High Range Water Reducer (HRWR) Visco Flow 10.

## MIX DESIGN

The mixing design ratio and techniques have been performed according to the method described by (fady et al., 2021) and (Kotb et al., 2021) [17,18].

### *Plain concrete mix design*

The compressive strength of concrete was designed to be 250 kg/cm<sup>2</sup> after 28 days. The method used for the concrete mix design was the absolute volume method. Tab. (3) illustrates the plain concrete mix design.

Beam No.	Elevation of beam	Cross section
Beam 01		
Beam 02		
Beam 03		
Beam 04		
Beam 05		

Table 2: Strengthening scheme.



	Cement	Water	Fine aggregate	Coarse aggregate
Weight	300 kg	165 liters	770.5 kg	1155.75 kg
Ratio	1 %	0.55 %	2.57 %	3.85 %

Table 3: Plain concrete mix design.

*ECC mix design*

The mixing process has been performed according to the method described by (Zhou et al., 2012) to improve the fiber dispersion at the ECC mixture. A locally manufactured mixer has conducted the mixing with an electric motor of four horsepower. It offers the possibility to mix in two opposite rotation directions with a velocity varying from 600 to 4000 revolutions per minute.

Tab. (4) Explain the ECC mixture's contents per 1 m<sup>3</sup> are:

	1 m <sup>3</sup>	Ratio
Cement	600	1 %
Fly Ash	720	1.2 %
Silica Sand	480	0.8 %
Water	360	0.6 %
polypropylene fiber	22.5	2 % (Cement + Fly ash)
polyvinyl alcohol fiber	26	2 % (Cement + Fly ash)
HRWR (VISC FLOW 10)	12	2 %

Table 4: ECC mix design.

This section introduces the basic design theory of ECC composition materials to understand work hardening behavior better and crack formation in multiple cracks in PVA fiber reinforced cement composites. Extensive research has shown that the most basic properties of fiber-reinforced cement-based materials relate to the relationship between the average tensile stress  $\sigma$  across cracks and the uniform crack opening  $\delta$ , commonly referred to as the  $\sigma - \delta$  curve. The  $\sigma - \delta$  curve establishes the relationship between the composite composition and the tensile ductility of the composite. Recently, pseudo-strain hardening model conditions used as design guidelines for ECC material adjustment were categorized into initial crack stress and steady crack criteria as follows:

(1) First cracking stress criterion

In this case, the initial crack strength  $\sigma_{fc}$  should be less than the maximum fiber cross-linking capacity at each potential crack level  $\sigma_0$ . The first cracked area loses tensile strength due to fiber breakage or pulling out. The standard formula is:

$$\sigma_{fc} \leq \sigma_0 \tag{1}$$

(2) Steady-state cracking criterion

Based on a J-integral analysis of the resting crack, it was found that the presence of the resting crack is reflected in the energy balance provided by the following equation:

$$J_{tip} = \sigma_{ss} \delta_{ss} - \int_0^{ss} \sigma(\delta) d\delta \tag{2}$$

and



$$\sigma_{ss} \leq \sigma_0 \tag{3}$$

Here,  $J_{tip}$  is the toughness of the tip of the crack, and if the volume fraction of the fiber is less than 5%, it can be roughly estimated as the toughness of the cement-based matrix.  $\sigma_{ss}$  is the steady-state crack stress.  $\delta_{ss}$  is the crack opening corresponding to  $\sigma_{ss}$ . Eqns. (2) and (3) mean steady-state crack criteria. H. The toughness of the crack tip  $J_{tip}$  should be smaller than the complementary energy  $J_b$  calculated from the  $\sigma - \delta$  curve, as outlined in Fig. 3.  $J_{tip}$  is smaller than the hatched part  $J_b$ .

$$J_{tip} \leq \sigma_0 \delta_0 - \int_0^{\delta_0} \sigma(\delta) d\delta = J_b \tag{4}$$

If the absorbed energy in the rising phase of  $\sigma - \delta$  curve is insufficient or the crack tip toughness is too high, the steady-state cracking criterion is hard to be satisfied.

From the aforementioned words and the following graph, we can emphasize a physical property of ECC, which is its high ductility, as it appeared in the Fig. (1).

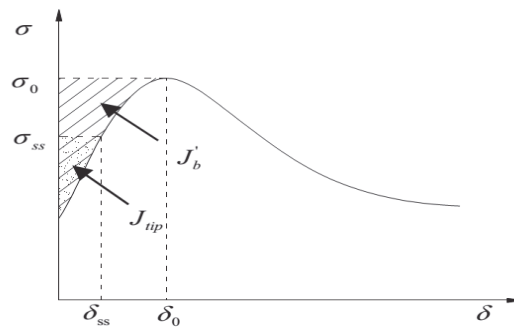


Figure 3: Typical relationship between fiber bridging stress and crack opening width.

## TEST METHODS

### *The compressive strength [18]*

In this paper, the compressive strength for plain concrete is equal to 25.11 MPa, and the compressive strength for the ECC matrix is equal to 41.17 MPa.

### *The tensile strength [18]*

In this paper, the tensile strength for plain concrete is equal to 1.89 MPa, and the tensile strength for the ECC matrix is equal to 8.91 MPa.

### *Flexural behaviour of ECC layered reinforced concrete beams*

The four-point load test is applied on the reinforced concrete beams on the effective span of 1300 mm, and tests have been carried out at room temperature and as per standards. Fig. (4) shows the dimension parameters, reinforcement details and position of the ECC layer.

Linear variable differential transformers (LVDT) are placed at mid span. LVDT and Load cell are connected to the data acquisition system. The readings and data are reordered and stored with the help of a computer. Using bending tests, parameters such as load bending curves, profile energy absorption, and displacement ductility are evaluated, and profile energy absorption is calculated by measuring the region between the yield and fracture points. Strain gauges (SG) are placed at the mid-span of the beam body at the bottom and put at the bottom steel bar and strengthen steel bar to read the strain of materials compared to loads as shown in Fig. (4).





Fig. (5) shows the four-point load test setup on the beam body. The Push pulls hydraulic jack of 1000 KN capacity is used to apply load on the four-point load setup of beam, below which load cell is placed and used to measure the applied load on the beam.

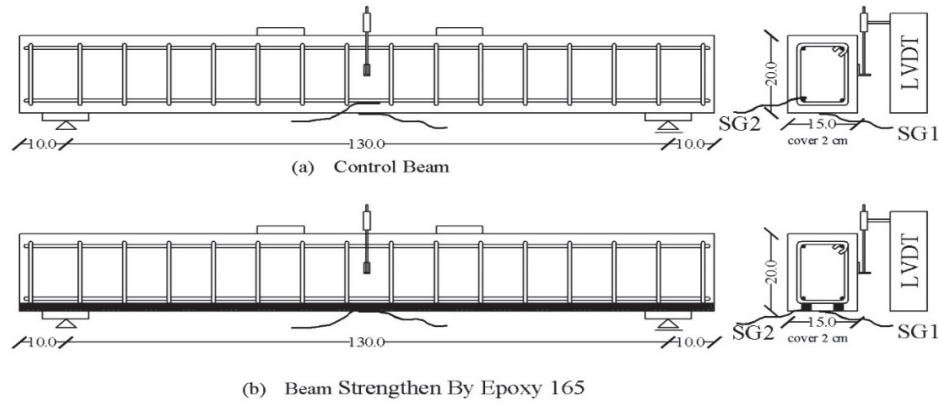


Figure 4: Strain gauges location and LVDT.

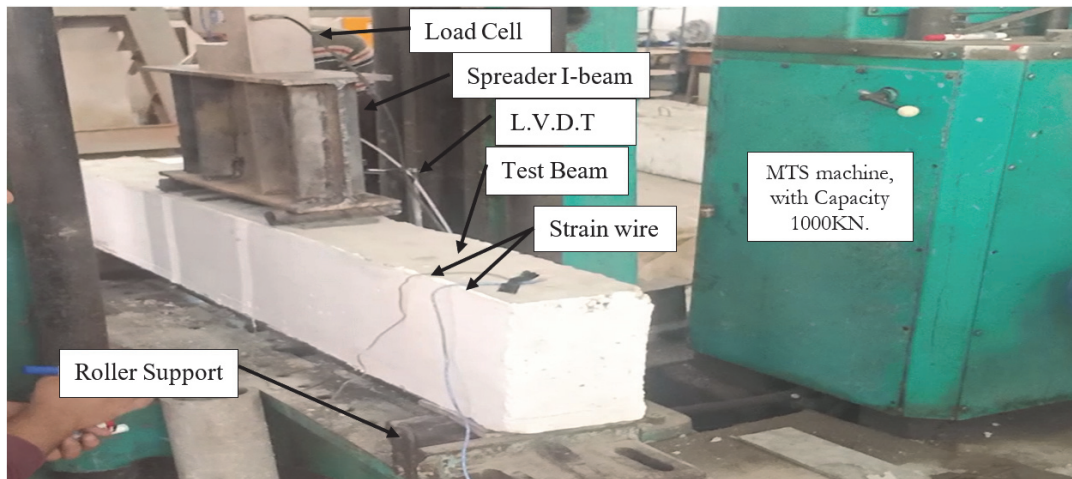


Figure 5: Four-point load test setup on beam.

## EXPERIMENTAL RESULTS

### *Load – Deflection Curve*

The four-point bending test was performed on a 1.5 m long reinforced concrete girder to investigate bending behavior, load-deformation curves, shown initial cracks, yield strength, load-bearing capacity, and fracture level. Fig. (6) shows the flexural behavior of the ECC layered beam under ultimate loading, and Tab. (5) shows the features of load deflection values such as the first crack, yielding, ultimate, and failure. as shown as Fig. (7).

Up to the yield point, all beams operated with similar performance under bending, and the first cracks occurred at all mixes in the stretching stage. After the compliance phase, a crack occurred between the load position/midfield of the beam. This may be due to the load characteristics of the beam. The hardened properties of ECC mixes under tensile/flexural load ensured that the load does not decrease rapidly after the initial crack and the brittle mode of failure of ECC-layered beams is different from convention beams. The strain property of ECC-layered beams is notable.

Multiple finer cracks formed in the tensile surface of the beam after flow slightly affect the strength, durability, and performance of the structure. The incidence of cracks increased with the rise in flexural load in all the specimens.

However, at a specific point, the creation of new cracks in the beam has not improved. The load-deflection curves for layered beams are more significant than the standard concrete curve, owing to ECC mixes' more excellent ductility quality. Fig. (7) shows the load-deflection curve for various beams. From the experimental results, it is observed that there has been a noteworthy development in beams with ECC layers.

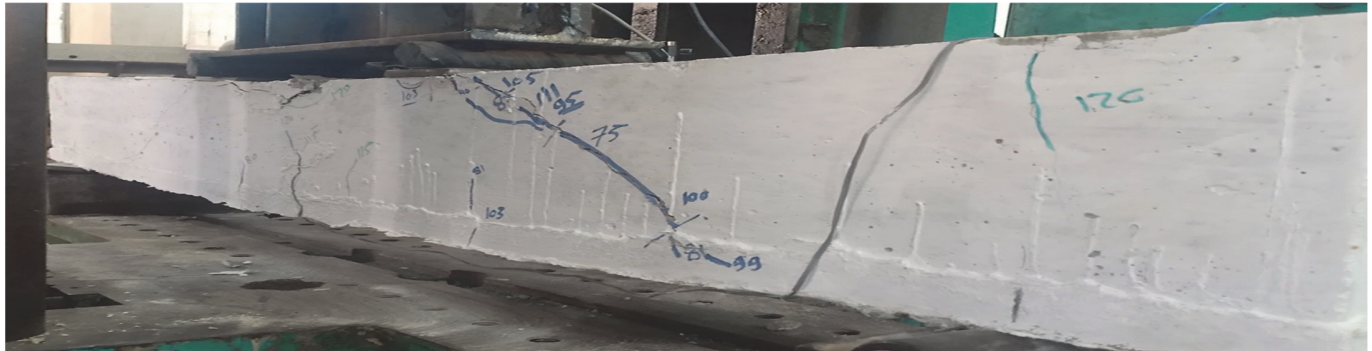


Figure 6: The flexural behavior of ECC layered beam under ultimate loading.

Beam No.	First Crack Load (KN)	Deflection @ First Crack (mm)	Yield Load (KN)	Deflection @ Yield Load (mm)	Ultimate Load (KN)	Deflection @ Breaking Load (mm)
Beam 01	3.5	0.39	14.4	1.582	27.9	9.271
Beam 02	18.2	0.97	101.7	7.938	107.55	10.519
Beam 03	3.335	0.71	.....	.....	108.6	10.65
Beam 04	1.6	0.294	133.8	12.294	142	19
Beam 05	3.6	0.893	.....	.....	148	12.4

Table 5: Features of load deflection values such as first crack, yielding, ultimate and failure.

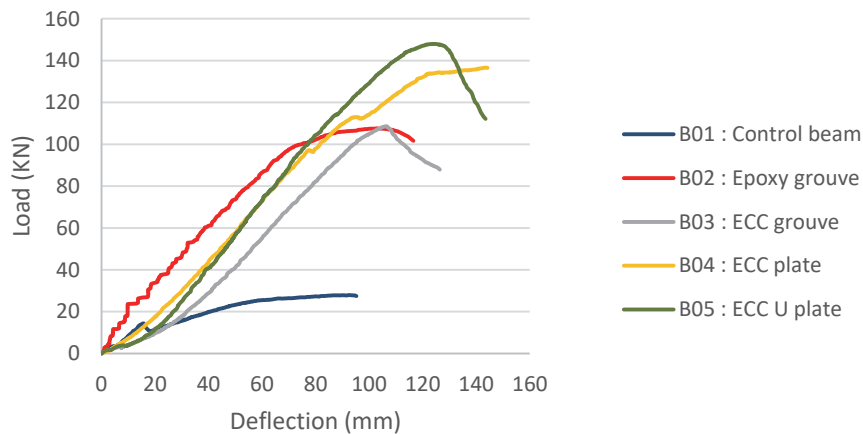


Figure 7: Load deflection curve for various beams.

*Load – (Concrete/ECC/Steel strain) Curve*

Fig. (4) illustrates strain location at the mid-span of the steel bar and the beam body. Strain readings were recorded from the attached strain gages during testing a data gaining system. Fig. (8A, 8B) shows the load versus concrete/steel strain for the strengthened beams.

*Crack patterns and failure modes*

Figures below show all tested beams' crack patterns and failure modes; some of the tested girders failed due to compound failure (flexural, Rupture, and shear). In general, the cracks start in the middle of the lower span; then, the number of these cracks increases, and as the applied load increases, another crack near the support appears to break down gradually.

Crack failure model for tested beam (B01) as shown in Fig. (9). In a typical model, the control beams failed after the longitudinal steel reinforcement yielded, resulting in concrete crushing. The vertical flexural crack was first initiated within the constant moment region at a load level of around 15 KN. The ultimate load with which the concrete beam was broken was 28 KN. Shear diagonal cracks were not observed in this series of bending tests. The type of failure incident is Flexural Failure.

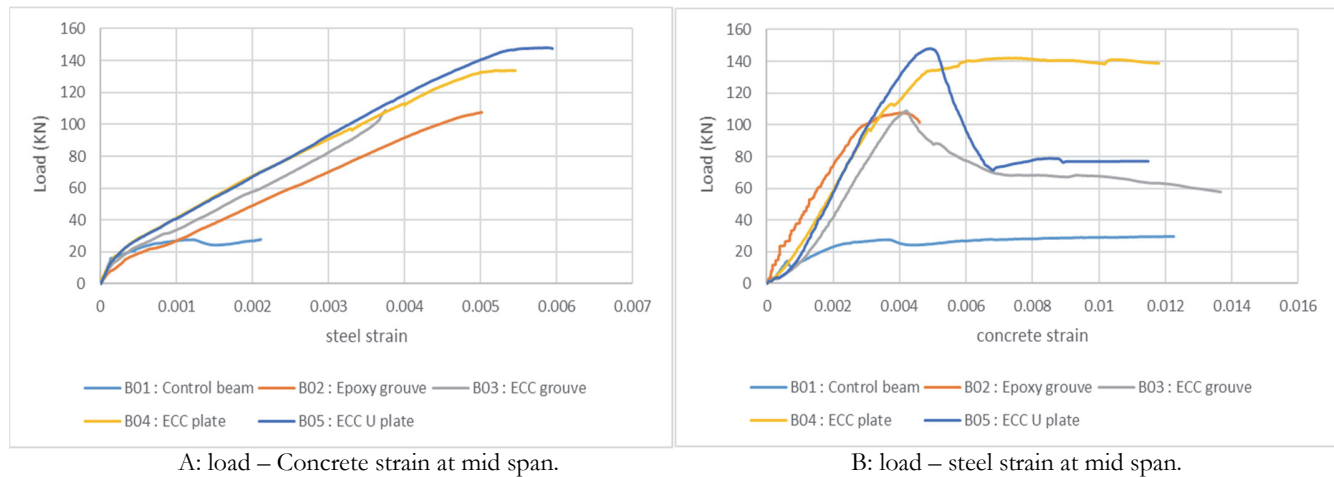


Figure 8: Load – Strengthening strain gages reading curve.

Crack failure model for tested beam (B02) as shown in Fig. (11,12). Initial cracks occurred in the epoxy mortar at a load level of (35) KN, and the ultimate load with which the concrete beam was broken was 109 KN. the epoxy mortar had a very high tensile strength. The local crack-induced debonding of the external strengthening groove was the failure mode of these reinforced beams. The epoxy groove Separated from the concrete beam body as shown in Fig. (10). The type of failure incident is **Flexural - Shear crack-induced debonding failure**.

Crack failure model for tested beam (B03) as shown in Fig. (14,15). Initial cracks occurred in the ECC mortar at a load level of (50) KN, and the ultimate load with which the concrete beam was broken was 106 KN. The failure mode of these strengthened beams was described as the tensile rupture of the external strengthening groove. Fig. (13) explains ECC groove rupture at tension surface. The failure incidents are **Flexural – Shear crack induced debonding failure and Rupture failure at the ECC groove**.

Crack failure model for tested beam (B04) as shown in Fig. (16,17). Initial cracks occurred in the ECC mortar at a load level of (75) KN, and the ultimate load with which the concrete beam was broken was 120 KN. The failure mode of these strengthened beams was described as the tensile rupture of the external strengthening plate. Figs. (18) explain ECC plate rupture at the tension surface. The types of failure incidents are **Flexural failure, Rupture failure at ECC plate, and compression failure**.

Crack failure model for tested beam (B05) as shown in Fig. (19). Initial cracks occurred in the ECC mortar at a load level of (72) KN, and the ultimate load with which the concrete beam was broken was 130 KN. The failure mode of these strengthened beams was described as the tensile rupture of the external strengthening block. Figs. (20) explain ECC block rupture at the tension surface. The types of failure incident are critical diagonal **crack-induced debonding, rupture failure at ECC plate, and compression failure**.

From previous results, it was found that:

- The results of the beams (B02 & B03) reinforced using epoxy and ECC mortar materials are approximate in the same strengthen the method and experiments have proven that these beams can withstand 3 times that of the control beam.
- And from practical experiments, it was found that the last method of reinforcement, which is (2Ø12 + ECC U-plate (5\*2) + (2\*15\*100) cm.), is the best in terms of carrying the beam to high loads and the method of its failure.
- A typical mode of failure of under-reinforced concrete beams was observed in the case of the beam (B04), where the crack started at the critical section (mid-span), which is near the constant moment region, and then transferred to the strengthened section.
- There was no secession between the material used in the Strengthen (ECC) and the concrete structure of the beam, unlike the use of epoxy materials.

- The behavior of the new material used in the reinforcement (ECC) is similar to the previously known reinforcement material (epoxy materials).
- The strengthened beams results illustrated that RC beam flexural strength varies by the shape of the strengthen method (ECC groove (2\*2\*100) cm, ECC plate (2\*15\*100) cm, and ECC U-plate (5\*2) + (2\*15\*100) cm) increased the ultimate load of the strengthened RC beams by about 73.58%, 76.67%, and 78.46% respectively.

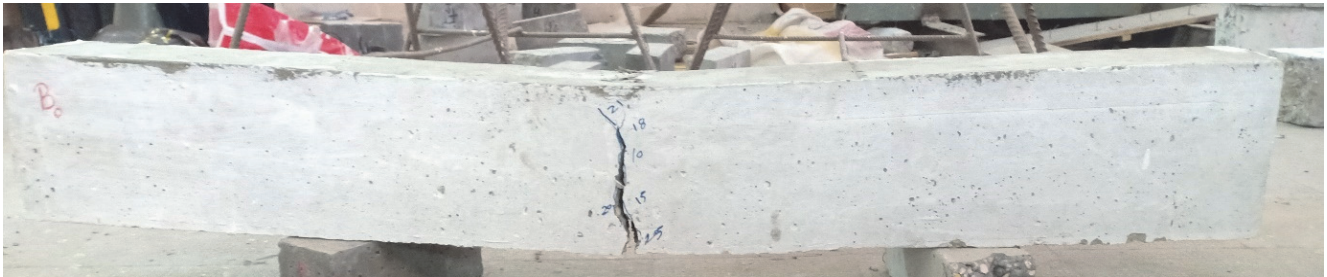


Figure 9: Concrete crack patterns at control beam.



Figure 10: Epoxy groove split from beam.



Figure 11: Concrete crack patterns at Epoxy beam (B 02).



Figure 12: Concrete crack patterns at Epoxy beam (B 02) Explain the resulting cracks.



Figure 13: ECC groove rupture at tension surface.



Figure 14: Concrete crack patterns at ECC beam (B 03).



Figure 15: Concrete crack patterns at ECC beam (B 03) explain ECC groove rupture at tension surface.



Figure 16: Concrete crack patterns at ECC beam (B 04) right side.



Figure 17: Concrete crack patterns at ECC beam (B 04) left side.

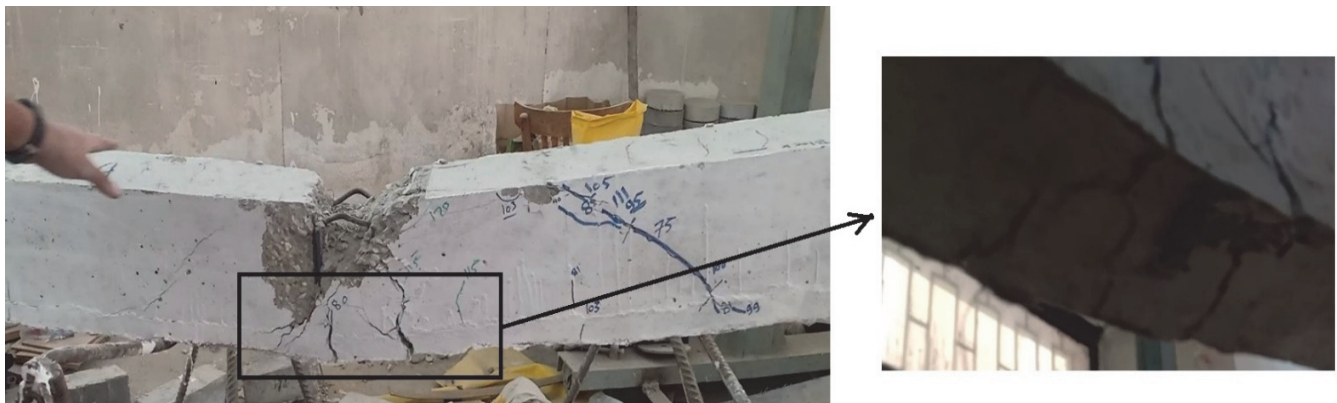


Figure 18: Concrete crack patterns at ECC beam (B 04) explain ECC plate rupture at tension surface.



Figure 19: Concrete crack patterns at ECC beam (B 05).

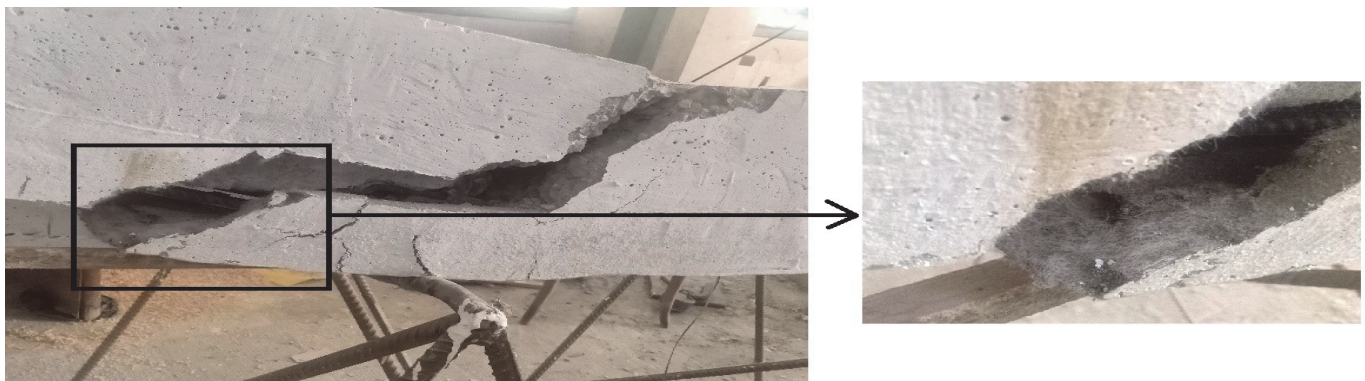


Figure 20: Concrete crack patterns at ECC beam (B 05) explain critical diagonal crack-induced debonding, Rupture failure at ECC plate and compression failure.

## NUMERICAL MODELLING

To define the malfunction of the nonlinear finite element model, the ANSYS 19.2 software was used. The software can work with complex numerical equations designed to accommodate the nonlinear course of action of concrete and ECC beams working under unchanging loads. The ECC beams were modelled by using SOLID 65 elements. These components require eight nodes at each node with three degrees of independence and x-, y- and z-direction nodal transformations. The properties of plastic deformation, three-dimensional cracking, and crushing of SOLID 65 components are. To simulate concrete behaviour, ANSYS utilizes linear isotropic and multi-linear isotropic material attributes for modeling concrete, along with additional concrete material properties.

### *Nonlinear Finite Element Analysis*

Nonlinear finite element method NLFEM analysis was conducted to compare with the experimental work results. This comparison aims to confirm the accuracy of the analysis and model. There is an excellent agreement between the

experimental and numerical load-deflection curves for all loading stages, as shown in Fig. (21). The FE models predicted the load-carrying capability of RC beams. The validity and dependability of the FE models developed to replicate experimental performance [16].

*Geometry of the Beam*

The dimensions of the RC beam consider for this study is (1500 mm x150 mm x200 mm). The beam is simply supported with a hinge at one end and a roller at another end. Two-point loads are applied at one-third of the span. The details of the beam as shown in Fig. (4.a).

*Element Types*

The SOLID 65 is used for 3D modelling of concrete beams with or without rebars. Concrete is capable of cracking in tension and crushing in compression. ANSYS SOLID 65 is used to model the concrete, and LINK 180 is used to model the steel reinforcement with real constants 50.265.

*Material Properties [18,19]*

Tab. (6) presents the mechanical properties of the materials used in the numerical modeling.

Material	Properties	Data	Unit
Concrete	Compression strength	25.11	MPa
	Tensile strength	1.89	MPa
	Young's modulus, $E_c$	22048.35	MPa
	Passion's ratio	0.2	
ECC	Compression strength	41.17	MPa
	Tensile strength	8.91	MPa
	Young's modulus, $E_c$	30157.01	MPa
	Passion's ratio	0.25	
Reinforced Steel	Young's modulus, $E_s$	200000	MPa
	Yield stress, $f_y$	350	MPa
	Passion's ratio	0.3	
Epoxy resin	Young's modulus, $E_s$	3780	MPa
	Yield stress, $f_y$	30	MPa
	Passion's ratio	0.35	

Table 6: Material properties used in the numerical study.

*Numerical Results*

Tab. (7) presents the specimens, cross-section, deformation shape occurred, concrete crash shape. The ultimate breaking loads for the beams' specimens (B01, B02, B03, B04, and B05) was (28.87 KN, 112.63 KN, 115.79 KN, 143.96 KN, and 156.86 KN) respectively.

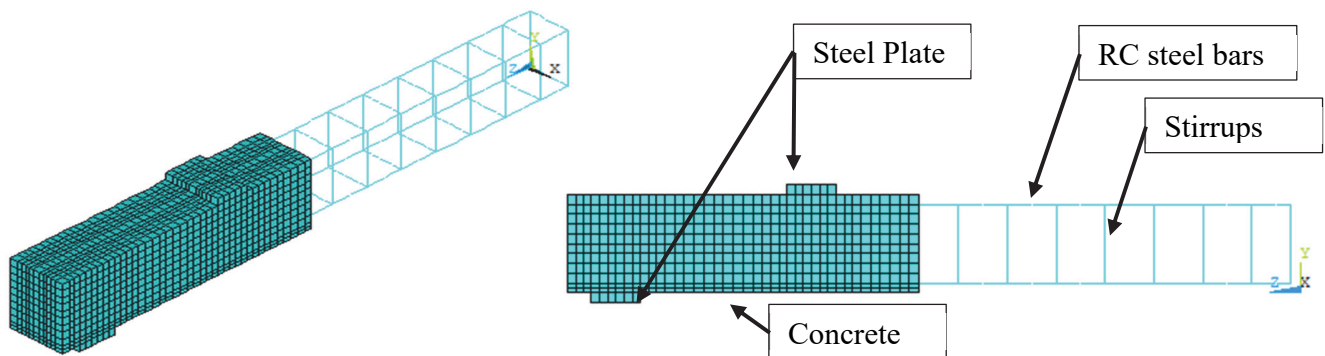


Figure 21: control beam (B01) ANSYS model.

No.	Cross section	Deformation shape	Concrete crash shape
B01			
<p style="text-align: center;">-7.06009    -6.13456    -5.20904    -4.28351    -3.35799    -2.43247    -1.50694    -.581418    .344106    1.26963</p>			
B02			
<p style="text-align: center;">-2.97998    -2.5764    -2.17282    -1.76924    -1.36565    -.962072    -.55849    -.154908    .248674    .652</p>			
B03			
<p style="text-align: center;">-2.95174    -2.5517    -2.15166    -1.75161    -1.35157    -.95153    -.551488    -.151446    .248596    .648639</p>			
B04			
<p style="text-align: center;">-4.01911    -3.4748    -2.93048    -2.38617    -1.84185    -1.29754    -.753225    -.20891    .335405    .87972</p>			
B05			
<p style="text-align: center;">-4.49688    -3.88963    -3.28238    -2.67513    -2.06788    -1.46064    -.853387    -.246138    .36111    .968359</p>			

Table 7: Numerical Results.





## COMPARISON OF EXPERIMENTAL AND NUMERICAL RESULTS

### Load – Deflection Curve

The load-deflection curves obtained for specimens from the experimental results and the FE models are shown in Fig. (22). It is clear that the experimental and numerical load-deflection results were in good agreement. So, the FE models demonstrated the ability to simulate the behavior of reinforced concrete beams strengthened by the NSM technique. The simulation perfectly reflected the bonding between concrete, steel reinforcement, and strengthening by NSM-steel rods. Moreover, the FE models result in confirming to affect the flexural capacity of beams strengthened with alteration of the strengthened cross-section.

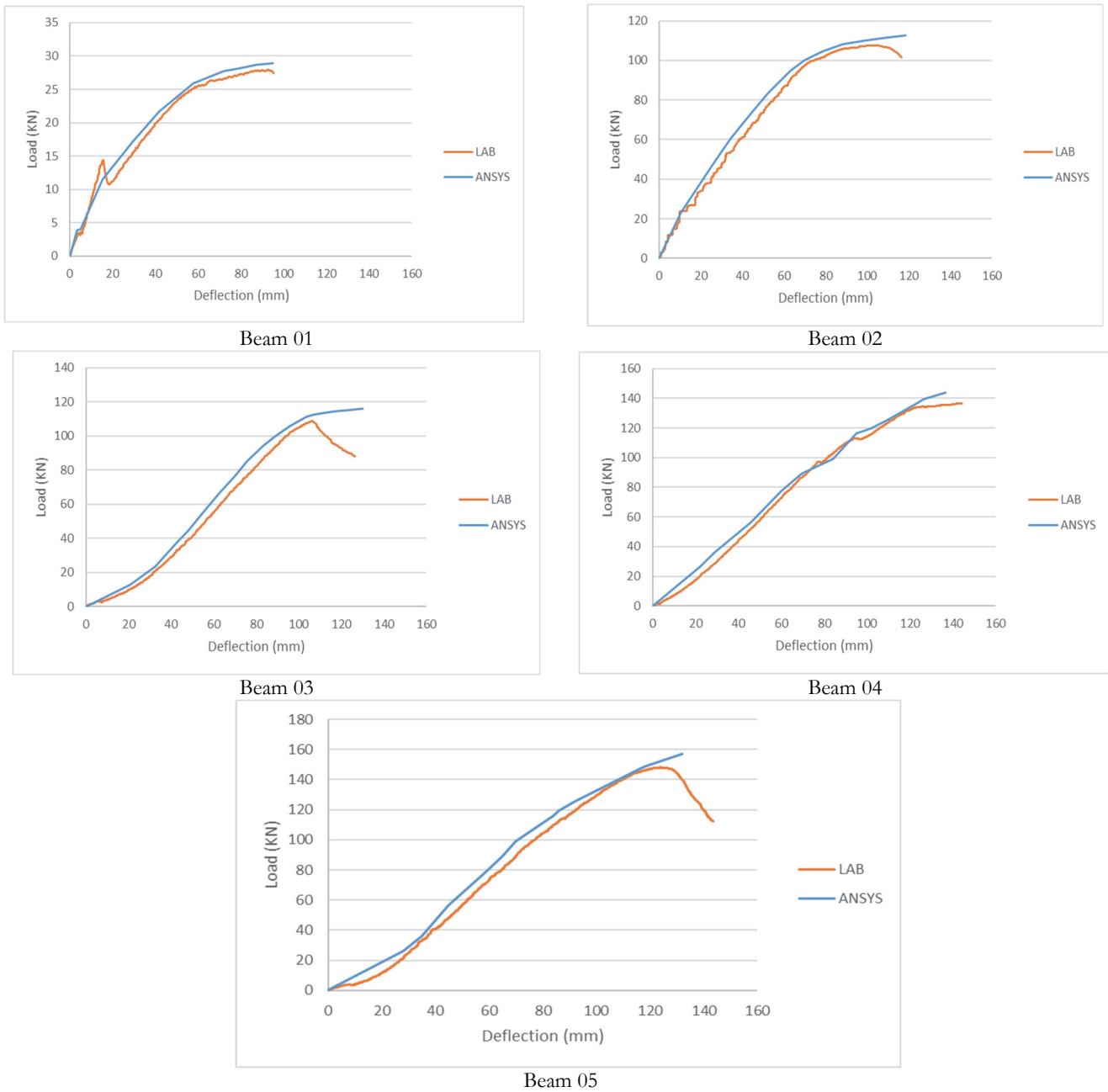


Figure 22: Comparison between experimental and numerical results.



## CONCLUSION

ECC has many attractive properties. A unique is the high tensile ductility several hundred times that of concrete while maintaining the compressive strengths similar to concrete or high strength concrete. The incidence of cracks increased with the rise in flexural load in all the specimens. ECC's metal-like behaviour is accomplished without relying on high fiber content, thereby breaking the conventional awareness of the need for a high fraction of fiber volume to attain high material efficiency. The moderate fiber content (2% or less by volume) makes ECC easily adaptable to construction project execution in the field or precast plant structural element production. Indeed, ECC has a proven variety of manufacturing pathways, including self-consolidating casting and spraying on-site, as well as pre-casting and extrusion off-site. It is apparent that retaining a relatively low fiber content is also necessary for economic reasons. Based on the above paper, we can conclude as follows:

- The compressive strength of ECC increases with an increase in cementitious material fly ash, silica sand, polypropylene fiber, polyvinyl alcohol fiber, etc.
- Using cement replacement materials and polyvinyl alcohol fibers resulted in a superior enhancement in the ductility performance. Especially the combination of 120% fly ash and 80% silica sand resulted in 85% enhancement in splitting tensile strength of ECC mortars.
- The large tensile ductility of ECC allows it to deform compatibly and creates a synergistic load-sharing capability with steel reinforcement in structural members. As a result, steel reinforcements in ECC members are better utilized in enhancing structural performance. Simultaneously, the tight crack width of the ECC protects the steel reinforcement from typical corrosive processes, resulting in improved structural durability.
- The ECC mortar can be used to increase the shear capacity of reinforced beams as an effective strengthening material.
- Ductility, resilience, compressive strength, and self-consolidation are the important properties of ECC Concrete.

This experimental study explores the possibilities of using ECC by strengthening RC beams with ECC plastic hinges and ECC layers in structural rehabilitation applications. A new generation of ECC material that embodies the advantages of both steel (ductility) and concrete can be expected to be developed. These new materials will be designed to achieve targeted structural performance levels.

- ❖ Sustainable with respect to social, economic and environmental dimensions.
- ❖ Self-healing when damaged.
- ❖ Functional to meet requirements beyond structural capacity.

## REFERENCES

- [1] Gadhiya, S., Patel, T.N., Shah, D. (2015). Bendable concrete: a review, 4.
- [2] Gohil, D.K.B.P. (2016). Study on Engineered Cementitious Composites with Different Fibres: A Critical Review, *Int. J. Innov. Eng. Technol.*, 6(3), pp. 5–9.
- [3] Zhou, J., Qian, S., Ye, G., Copuroglu, O., Van Breugel, K., Li, V.C. (2012). Improved fiber distribution and mechanical properties of engineered cementitious composites by adjusting the mixing sequence, *Cem. Concr. Compos.*, 34(3), pp. 342–348, DOI: 10.1016/j.cemconcomp.2011.11.019.
- [4] Şahmaran, M., Li, V.C. (2009). Durability properties of micro-cracked ECC containing high volumes fly ash, *Cem. Concr. Res.*, 39(11), pp. 1033–1043, DOI: 10.1016/j.cemconres.2009.07.009.
- [5] Kan, L.L., Shi, H.S. (2012). Investigation of self-healing behavior of Engineered Cementitious Composites (ECC) materials, *Constr. Build. Mater.*, 29, pp. 348–356, DOI: 10.1016/j.conbuildmat.2011.10.051.
- [6] Zhang, J., Wang, Z., Ju, X. (2013). Application of ductile fiber reinforced cementitious composite in jointless concrete pavements, *Compos. Part B Eng.*, 50, pp. 224–231, DOI: 10.1016/j.compositesb.2013.02.007.
- [7] Qian, S.Z., Zhou, J., Schlangen, E. (2010). Influence of curing condition and precracking time on the self-healing behavior of Engineered Cementitious Composites, *Cem. Concr. Compos.*, 32(9), pp. 686–693, DOI: 10.1016/j.cemconcomp.2010.07.015.
- [8] Jen, G., Ostertag, C.P. (2016). Experimental observations of self-consolidated hybrid fiber reinforced concrete (SC-HyFRC) on corrosion damage reduction, *Constr. Build. Mater.*, 105, pp. 262–268, DOI: 10.1016/j.conbuildmat.2015.12.076.
- [9] Jung, W.T., Park, Y.H., Park, J.S., Kang, J.Y., You, Y.J. (2005). Experimental investigation on flexural behavior of RC



- beams strengthened by NSM CFRP reinforcements, *Am. Concr. Institute, ACI Spec. Publ.*, SP-230, pp. 795–805.
- [10] Novidis, D., Pantazopoulou, S.J., Tentolouris, E. (2007). Experimental study of bond of NSM-FRP reinforcement, *Constr. Build. Mater.*, 21(8), pp. 1760–1770, DOI: 10.1016/j.conbuildmat.2006.05.054.
- [11] Yang, Y., Lepech, M.D., Yang, E.H., Li, V.C. (2009). Autogenous healing of engineered cementitious composites under wet-dry cycles, *Cem. Concr. Res.*, 39(5), pp. 382–390, DOI: 10.1016/j.cemconres.2009.01.013.
- [12] Yang, E.H., Yang, Y., Li, V.C. (2007). Use of high volumes of fly ash to improve ECC mechanical properties and material greenness, *ACI Mater. J.*, 104(6), pp. 620–628, DOI: 10.14359/18966.
- [13] Vinoth Kumar, K.L., Karthikeyan, G. (2017). Experimental study on flexural response of engineered cementitious composite (ECC) strengthened reinforced concrete beams, *Int. J. Civ. Eng. Technol.*, 8(8), pp. 313–23.
- [14] Shang, X.Y., Yu, J.T., Li, L.Z., Lu, Z.D. (2019). Strengthening of RC structures by using engineered cementitious composites: A review, *Sustain.*, 11(12), DOI: 10.3390/su10023384.
- [15] Kim, J.K., Kim, J.S., Ha, G.J., Kim, Y.Y. (2007). Tensile and fiber dispersion performance of ECC (engineered cementitious composites) produced with ground granulated blast furnace slag, *Cem. Concr. Res.*, 37(7), pp. 1096–1105, DOI: 10.1016/j.cemconres.2007.04.006.
- [16] Ibrahim, Y.E., Fawzy, K., Farouk, M.A. (2021). Effect of steel fiber on the shear behavior of reinforced recycled aggregate concrete beams, *Struct. Concr.*, 22(3), pp. 1861–1872, DOI: 10.1002/suco.202000494.
- [17] Husain, M., Fawzy, K., Kotb, K.F. (2019). Khaled Fawzy and Khaled Fawzy Kotb, Sway of Steel Fiber and Recycled Aggregate Content on Mechanical Properties of Recycled Aggregate Concrete, *Int. J. Civ. Eng. Technol.*, 10(03), pp. 3067–3078.
- [18] Awad, F., Hussein, M., Fawzy, K. (2021). ICESA 2021 Second International Conference for Engineering Sciences and Applications Study of the Mechanical Properties of Engineered Cementitious Composites (ECC) using experimental and numerical analysis.
- [19] El-Emam, H., El-Sisi, A., Reda, R., Seleem, M., Bneni, M. (2020). Effect of concrete cover thickness and main reinforcement ratio on flexural behavior of RC beams strengthened by NSM-GFRP bars, *Frat. Ed Integrita Strutt.*, 14(52), pp. 197–210, DOI: 10.3221/IGF-ESIS.52.16.